International Journal of Applied Pharmaceutics

ISSN- 0975-7058 Vol 18, Issue 2, 2026

Original Article

DEVELOPMENT AND EVALUATION OF A PH-RESPONSIVE OFLOXACIN-LOADED NANOPARTICLE *IN SITU* GEL FOR SUSTAINED OCULAR DELIVERY

MARGRET CHANDIRA RAJAPPA[1*], GRACY GLADIN SOLOMON[2], NAGASUBRAMANIAN VENKATASUBRAMANIAM[3], MANOJ KUMAR KUMAR[3], DHARSHINI VELMURUGAN[4]

[1,3,4]Vinayaka Mission's College of Pharmacy, Vinayaka Mission's Research Foundation (DU), Ariyanoor, Salem-636308, India. [2]Department of Pharmaceutics, School of Pharmacy, Sri Balaji Vidyapeeth Deemed to be University, Puducherry, Cuddalore Road, Pillaiyarkuppam, Puducherry-607402, India.

[*]Corresponding author: Margret Chandira Rajappa; [*]Email: mchandira172@gmail.com

Received: 21 Oct 2025, Revised and Accepted: 24 Jan 2026

ABSTRACT

Objective: This study aims to develop an *in situ* gel formulation incorporating Ofloxacin-loaded nanoparticles to enhance ocular residence time and therapeutic efficacy of drug.

Methods: The formulation process included pre-formulation studies such as solubility and UV analysis of Ofloxacin. A pH-triggered *in situ* gel was prepared using Poloxamer 407, chitosan, and Eudragit L-100. Various post-formulation parameters were evaluated, including pH, viscosity, drug content, and *in vitro* drug release kinetics.

Results: Nanoparticles were confirmed using DLS with a particle size of 688 nm. The viscosity of *in situ* gel formulations followed a shear thinning process before contact with simulated tear fluid (STF). The viscosity reduced significantly ($p<0.05$, two-way ANOVA) for the *in situ* formulations after contact with STF. The formulation containing 4% Poloxamer 407 and 0.8% Gellan Gum (OFX3) demonstrated acceptable viscosity behavior and sustained drug release. OFX3 achieved a drug release of 97.81% over 6 h, adhering to Higuchi release models and expressing quasi-Fickian diffusion. The HET-CAM test confirmed the formulation non-irritant nature, while stability studies demonstrated no significant changes over a 3-month period.

Conclusion: The developed pH-sensitive *in situ* gel effectively enhances the solubility of Ofloxacin, providing a promising treatment option for bacterial conjunctivitis. The developed ofloxacin-loaded nanoparticulate *in situ* gel successfully integrates controlled release through prolonged ocular residence. Future *in vivo* studies will further consolidate its potential as a pioneering candidate for translational ophthalmic applications.

Keywords: Bacterial conjunctivitis, pH Triggered polymer, Nanoparticle, *In situ* gel, HET-CAM test

DOI: https://dx.doi.org/10.22159/ijap.2026v18i2.57216 Journal homepage: https://innovareacademics.in/journals/index.php/ijap

INTRODUCTION

Ocular conjunctivitis is a common allergic illness occurring in the eyes, often characterized by the inflammation due to allergens especially microbes [1]. This ocular illness accounts for two-thirds of the total ocular-based cases in pediatric populations [2]. According to a cross-sectional survey in 2023, attack rate of conjunctivitis is extremely high in households with a median attacking rate of 100% [3]. Conjunctivitis can be infectious or non-infectious in nature. Infectious conjunctivitis can cause loss of eyesight due to severe infection-induced corneal inflammation [4, 5]. Bacterial conjunctivitis is a common type of bacterial infection affecting all age groups irrespective of sex [6].

Ofloxacin is a promising fluoroquinolone known for its broad-spectrum activity especially expressing more than 60% anti-bacterial activity against *Staphylococcus aureus* and g-negative bacterial strains [6, 7]. However, lack of sub-optimal concentrations in ocular surface causes antibiotic resistance against ofloxacin [8]. Antibiotic resistance in eye is serious apprehension, which is capable of causing high mortality, up to 10 million by 2050 in case of not treating properly [9].

The drug release in the affected area of eye is limited under inflammatory conditions due to excessive defensive mechanisms like tear secretion [10]. Minimal retention of nanoparticles within the ocular region is the major drawback of ocular delivery. This is due to the clearance of drug by the blood and lymph flow to the eyes, especially under inflammatory and infectious conditions [11, 12]. Hence, larger particle size range is required to enhance the retention and prolong the residence time in *cul-de-sac* [13]. Chitosan-based nanoparticles obtained in the range of 200-600 nm expressed extended ocular residence time in *cul-de-sac* [14].

The above condition can be addressed by this research by employing *in situ* gel model, which gels from liquid state once administered inside the eye. The main aim of this research is to prolong the ocular residence of the drug through sustained drug delivery. Nanoparticles will help in preserving the drug from enzymatic reactions within the ocular region [15]. This *in situ* gel model will be highly helpful since *in situ* gels can be administered as eye drops, which improves the patient compliance and adherence. Because, eye ointments are less compliant by the patients despite the higher bioavailability than eye drops [16, 17]. Ease of application is an advantage for eye drops making patients self-efficacious, which remains in case of *in situ* gels [18, 19].

MATERIALS AND METHODS

Chemicals and reagents

Ofloxacin (CAS: 82419-36-1) was obtained as a gift sample from Shilpa Medicare Limited, Bangalore. Chitosan (CAS: 9012-76-4), Eudragit l-100 (CAS: 25086-15-1), Sodium chloride (CAS: 7647-14-5), Sodium bicarbonate (CAS: 144-55-8), Potassium chloride (CAS: 7447-40-7) was obtained from Oxford Laboratories, Maharastra. Poloxamer 407 (CAS: 9003-11-6) was purchased from Jignesh Agency Pvt Ltd, Maharashtra. Acetone (CAS: 67-64-1) was obtained from Pallav Chemicals, Tarpur. Gellan Gum (CAS: 71010-52-1) was purchased from Suvidhinath Laboratories, Vadodara. Polyvinyl alcohol (CAS: 9002-89-5) was obtained from Nice Chemicals, Cochin. Carbopol 943 (CAS: 9003-01-4) was obtained from Molychem, Mumbai. Benzalkonium Chloride (CAS: 63449-41-2) was bought from Loba Chemie, Maharastra.

Methods

Organoleptic characterization and solubility studies

A small sample of the pure drug was spread on white paper to observe its physical characteristics (e. g., color, texture). [20] The solubility of ofloxacin was tested using different solvents. Ethanol,

water, chloroform, and dimethyl sulphoxide (DMSO) were some solvents, which were used in this study [21].

UV-vis spectrophotometric analysis

100 mg of pure drug was initially dissolved in sufficient amount of ethanol. The first stock solution (100 µg ml^{-1}) was made by making the volume up with distilled water to 100 ml. Further dilutions were made up using distilled water. The second stock of 10 µg ml^{-1} was prepared by diluting 10 ml of 1st stock solution up to 100 ml. This stock solution was used to prepare aliquots of five different concentrations at 2, 4, 6, 8 and 10 µg ml^{-1}. The aliquots of ofloxacin were analyzed in the UV region (200-400 nm) to identify absorption maxima using UV-vis spectrophotometer (Systronics UV-2202, Systronics India Ltd., Ahmedabad, India) [22].

Drug–excipient compatibility studies

Fourier transform infrared (FT-IR) spectroscopy was used to study the interaction between ofloxacin and excipients. The samples for FT-IR spectroscopy were prepared by potassium bromide pelletization technique. Under this technique, sample were mixed with sufficient quantities of potassium bromide and was compressed using hydraulic press (Athena Technologies, Freemont, USA) and the resultant pellet was scanned in FT-IR spectrometer (Perkin Elmer Spectrum 1000 series, Massachusetts, United States) in the range of 4000 to 400 cm^{-1} [23].

Preparation of polymeric drug-loaded nanoparticles

Kesarla et al. (2016) [24] was adopted for preparation of nanoparticles with slight modifications. Predetermined quantity of ofloxacin (250 mg) and Eudragit (400 mg) were mixed with acetone (10 ml) and was made up to 50 ml with distilled water. This resultant solution was mixed in a homogenizer at 13000 rpm for 3 min. After homogenization, this organic solution was filtered and freeze-dried using a lyophilizer (Labman LMFD62, Labpro International, Haryana, India). In order to obtain the free flow particles, the lyophilized precipitate was collected as nanoparticles and passed through the sieve no. 120 [24].

Particle size

The particle size distribution of the ofloxacin nanoparticles solution was determined using a Zeta Sizer (Malvern Ver 8.02, Malvern Panalytical, Worcestershire, UK). The sample was well-dispersed to avoid undissolved particles. This analysis was conducted using distilled water as dispersant at 25 °C at 25 kcps after serial dilution to avoid multiple scattering. This analytical examination was performed for the API-loaded nanoparticles before incorporation into the *in situ* gel formulations [25].

Zeta potential

Zeta potential of the ofloxacin nanoparticles was measured using a Zeta Sizer (Malvern Ver 8.02, Malvern Panalytical, Worcestershire, UK) under 25 °C to assess particle stability and interactions before incorporation into the *in situ* gel. This analysis was conducted using as water as dispersant at 25 kcps [26].

Preparation of nanoparticle loaded *in situ* gel

After that, the poloxamer and gellan gum were weighed and mixed thoroughly, until a homogeneous liquid was achieved. Additionally, the produced nanoparticles were added to the solution mentioned above, thoroughly stirred for 30 min using a magnetic stirrer, and required quantity of Benzalkonium Chloride is added as Preservative. The composition of different *in situ* gel formulations (OFX1-OFX6). The ingredients along with their quantities are tabulated in *table 1* [24, 27].

Table 1: Formulation table for preparation of ofloxacin-loaded nanoparticles *in situ* gel

Ingredients	OFX1	OFX2	OFX3	OFX4	OFX5	OFX6
Ofloxacin (Nanoparticle) (%w/v) equivalent to 250 mg dose	250	250	250	250	250	250
Gellan gum (mg)	200	300	400	200	300	400
Poloxamer 407 (mg)	600	500	400	-	-	-
Carbopol 943 (mg)	-	-	-	600	500	400
Benzalkonium chloride (ml)	q. s	q. s	q. s	q. s	q. s	q. s
Distilled water (ml)	q. s. (50 ml)	q. s. (50 ml)	q. s. (50 ml)	q. s. (50 ml)	q. s. (50 ml)	q. s. (50 ml)

pH measurement

A digital pH meter (Systronics µ-PH-361, Systronics India Ltd., Ahmedabad, India) was calibrated using triple point method (pH 4, 7, and 9). The pH of each formulation was measured at 25±0.5 °C [24].

Viscosity measurement

The viscosity of the formulations was measured at different speeds (50, 75, and 100 rpm) and at 37ºC using a viscometer (Labman LMDV-100, Labman Technolgies, North Yorkshire, UK) with Spindle No. 01. The value was noted before and after addition of simulated tear fluid [28].

Determination of drug content

Ocular *in situ* gel samples were diluted to a concentration of 10 µg ml^{-1} with methanol and made-up using water. Drug content was measured using double beam UV-vis Spectrophotometer (Systronics UV-2202, Systronics India Ltd., Ahmedabad, India), and the test was performed in triplicate [29].

***In vitro* diffusion studies**

Preparation of stimulated tear fluid

In a 100 ml volumetric flask, add 0.670 g of sodium chloride, 0.200 g of sodium bicarbonate, and 0.248 g of potassium chloride, and mix. Distilled water was used to dissolve and dilute the artificial tears fluid solution to volume. In contrast, sodium bicarbonate is used to raise the pH of the solution, whereas HCl is used to lower it.

Preparation of egg membrane

The egg membrane was used for investigations, with unbroken eggs selected and their shells carefully broken to form a hole. The membrane was soaked in concentrated HCl for 2 h and attached to a donor compartment containing 1 ml of the formulation, while the receptor compartment held 100 ml of simulated tear fluid (STF) at 35 °C. Samples (2 ml) were withdrawn at intervals up to 6 h and analyzed using double-beam UV spectroscopy to calculate drug release. Equal quantity of sample was replaced in the receptor compartment to establish the sink conditions [30, 31].

Release kinetics profiling

The release data from the manufactured ocular *in situ* gel were fitted into various kinetic models: zero-order, first-order, Higuchi model, Hixson-Crowell and Korsmeyer-Peppas model. This was performed to understand the mechanism of drug release. Fickian constant was calculated from Korsmeyer-Peppa's plot to identify the type of diffusion mechanism. The n-value was recalculated for the first 60% of the plot. The geometry of the plot was considered to be cylindrical shape [32].

Scanning electron microscopy (SEM)

SEM (Carl Zeiss EVO 18, Carl Zeiss Microscopy, UK) was used to analyze the particle size and composition of the optimized formulation. The sample was observed at 1 µm and 2 µm by placing the sample in sample holder of scanning electron microscope (Carl Zeiss EVO18). Image was further enhanced for improved

visualization by using ImageJ software. Extra high tension (EHT) was maintained at 10 kV with magnification at 16.80kx (1 µm) and 11.56 kx (2 µm) [33].

***In vitro* HET-CAM test**

The hen's egg chorioallantoic membrane (HET-CAM) test substitute's animal use in assessing severe ocular irritation. In this study, ten-day-old fertilized eggs (50-60 g) were incubated at 37ºC, rotating every 12 h. After examining for damage, three eggs were selected. The shell was cut (2×2 cm), and 1 ml of ofloxacin ocular *in situ* gel was applied to egg no. 01, while 0.9% NaCl served as the negative control (egg no. 02) and 1% NaOH as the positive control (egg no. 03). After application, the chorioallantoic membrane was observed for five minutes for hemorrhage, coagulation, and vessel changes, and an irritancy score was calculated [34].

$$\left[\left(\frac{301-(haemorrhage\ time)}{300}\right)\times 5\right]+\left[\left(\frac{301-(Lysis\ time)}{300}\times 7\right)\right]+\left[\left(\frac{301-(Coagulation\ time)}{300}\times 9\right)\right]$$

Equation 1: Calculation of Irritancy score for *in situ* gel

Where,

Hemorrhage Time = Observation in seconds of hemorrhage reactions on CAM

Lysis Time = Observation in seconds of vessels Lysis on CAM

Coagulation time = Observation in seconds of coagulation formation on CAM

Stability studies

Stability studies were conducted for the optimized formulation following ICH guidelines. In the current work, a three-month stability analysis for the optimized formulation was conducted at 40°C ±2 °C/75%RH±5%RH [35, 36].

Statistical analysis

One-way ANOVA was performed for pH, Drug Content and *in vitro* HET-CAM assay. For Viscosity and Drug Release profile, two-way ANOVA was performed. Based on Levene's test (to understand the normality of the distribution), Tukey's HSD test (Equal variance) (or) Games-Howell test (Unequal variance) was employed as a post-hoc analysis to identify statistically significant pairs.

RESULTS

Organoleptic characterization and solubility studies

The pure drug powder was pale yellow with faint medicinal odour and bitter taste. As for solubility, the API was highly soluble in certain organic solvents like ethanol and DMSO. Ofloxacin was poorly soluble in water and acetone.

UV-vis spectrophotometric analysis

The Absorption maximal peak was observed at 288 nm. Besides, the LOD and LOQ was calculated to be 0.055 µg ml^{-1} with a slope of 0.1825 µg ml^{-1} and minimal standard deviation of blank (σ = ±0.01). The calibration curve followed excellent linearity (R^2=0.9961) following Beer-Lambert's law. The UV spectrophotometric graph and calibration curve of the drug is shown in fig. 1.

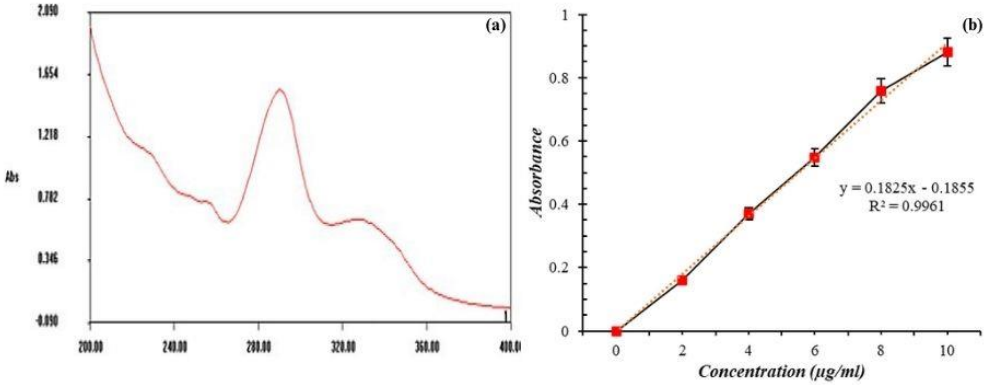

Fig. 1: UV-spectrophotometry containing (a) The UV spectrum of ofloxacin and (b) Linearity curve of Ofloxacin

Drug–excipient compatibility studies

A total of 9 distinct peaks were observed with the sharpest peak observed at 1850 cm^{-1}. The peak around 1049 cm^{-1} confirmed the presence of organic flouride moiety, confirming the monofluorinated structure of ofloxacin. Furthermore, multiple peaks like vibrations observed in the range between 3000 cm^{-1}and 3160 cm^{-1} confirmed the aromatic structure of ofloxacin. An aromatic hydroxyl group was confirmed by a prominent peak near 3400 cm^{-1}. The FT-IR spectrum of pure drug and physical mixture is shown in fig. 2.

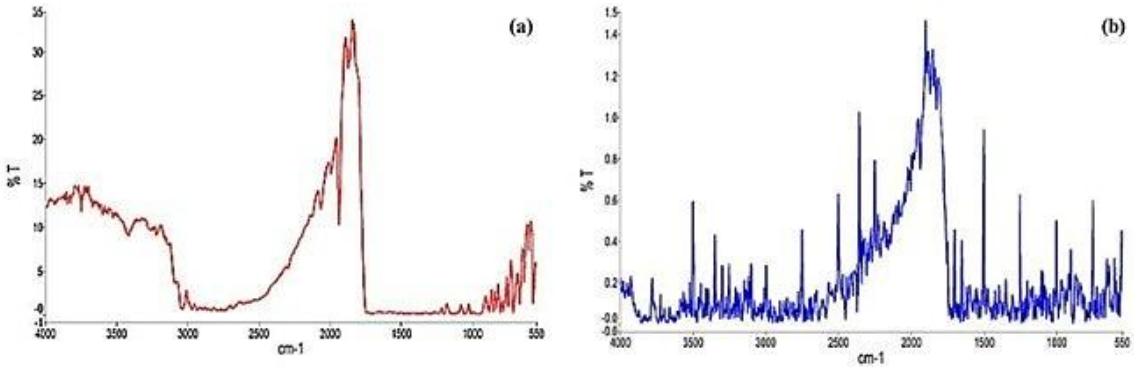

Fig. 2: FT-IR spectrum of (a) Pure drug (Ofloxacin) and (b) Physical mixture, there was no absence of existing peaks of API in the physical mixture, indicating the excellent compatibility of excipients with the API

Table 2: Significant peaks of API in FT-IR and their interpretations

Peak (cm^{-1})	±tolerance	Relative strength (image)	Likely assignment
3761	±15	weak–moderate	O–H free/overtone/combination band (weak OH stretch or artifact)
3326	±15	weak–moderate	Broad O–H and/or N–H stretching (carboxylic OH and/or piperazinyl N–H)
2026	±20	Weak	overtone/combination band or instrumental feature (not a typical fundamental for ofloxacin)
1850	±20	very strong	deep absorption — likely the quinolone/carbonyl region (C=O stretching(s) — note: carboxylic C=O typically ~1710–1760, quinolone/pyridone C=O can appear lower; here features may be merged/shifted)
1611	±15	moderate	C=C aromatic/C=O conjugated (aromatic ring stretch/amide-like C=O or quinolone C=O)
1196	±15	weak–moderate	C–O stretching/C–N stretch (fingerprint region)
1049	±15	Weak	C–O stretch/C–N stretch/C–F contribution region (fingerprint region)
845	±15	Weak	aromatic C–H out-of-plane bending (substituted aromatic ring)
599	±15	moderate	fingerprint region — C–F bending/ring deformation (fluoro-substituted ring features often occur here)

Particle size

The mean particle size of 688.1 nm (fig. 3), confirming the nanosize of the prepared particles. This particle size increased by approximately 50 nm after incorporation of nanoparticles in the *in situ* gel (737.7 nm). The DLS size distribution appeared monomodal, although the elevated PDI (>0.3) suggests broad particle size distribution and possible associative structures/aggregation. The monomodal graph was observed even after the incorporation of the nanoparticles into in the formulation. The poly-dispersibility Index (PDI) was greater than 0.3 after the incorporation of the nanoparticles, which may be due to the agglomeration of the nanoparticles within the porous networks of *in situ* gel formulation.

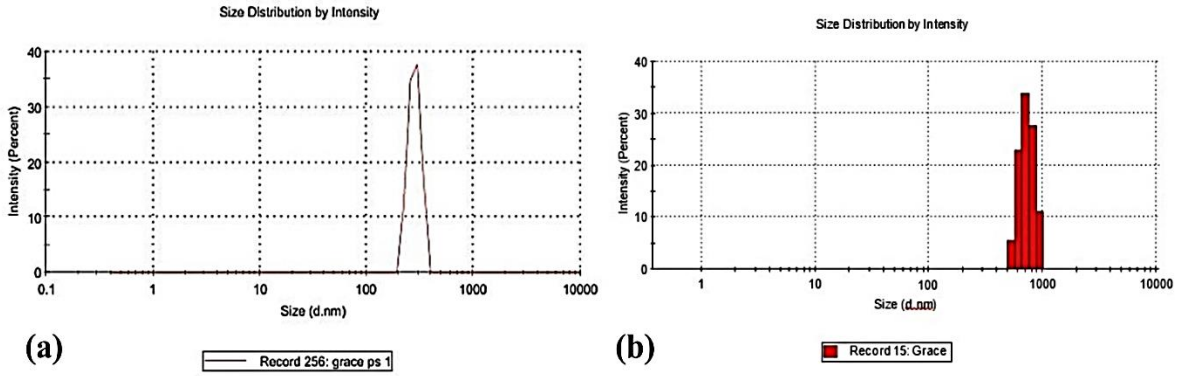

Fig. 3: Particle size distribution of (a) Ofloxacin-loaded nanoparticles (b) Nanoparticles incorporated *in situ* gel

Zeta potential

The mean zeta potential of nanoparticles was calculated to be-33.9 mV (fig. 4). This indicates the high stability of monomodal system observed in terms of surface electric charge. The standard deviation of the observed peak was ±6.93 mV.

pH measurement

The pH of formulations was weakly acidic to weakly alkaline ranging between 6.8-7.5. The formulations of poloxamer 407 (OFX1) were slightly more acidic than that of carbopol 943. The pH of different formulations is graphically represented in fig. 5.

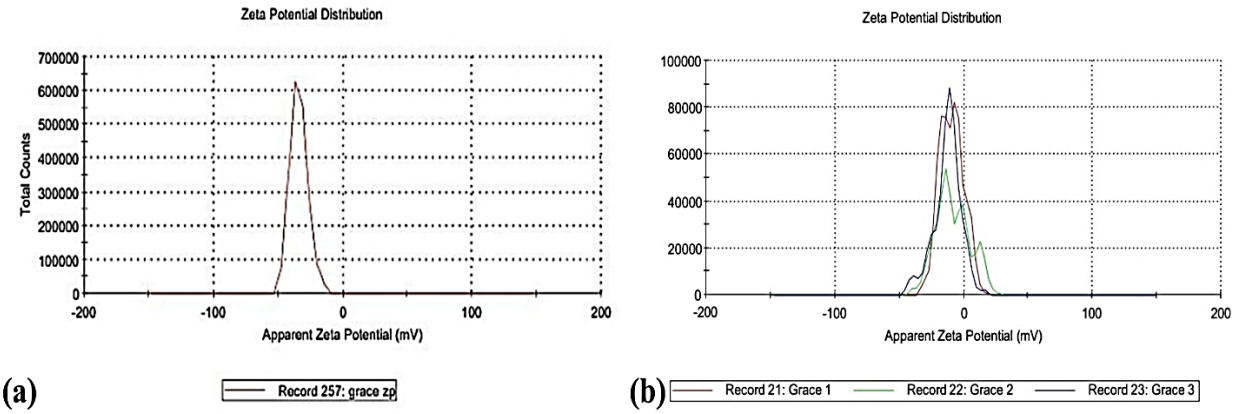

Fig. 4: Zeta potential of (a) Ofloxacin-loaded nanoparticles (b) Nanoparticles incorporated *in situ* gel, the zeta potential of the nanoparticle-loaded *in situ* gel was increased (-9.42 mV) compared to the drug loaded nanoparticles before the incorporation process. This is possible due to neutralization of the surface charge of nanoparticles by the positivity charged polymer matrix

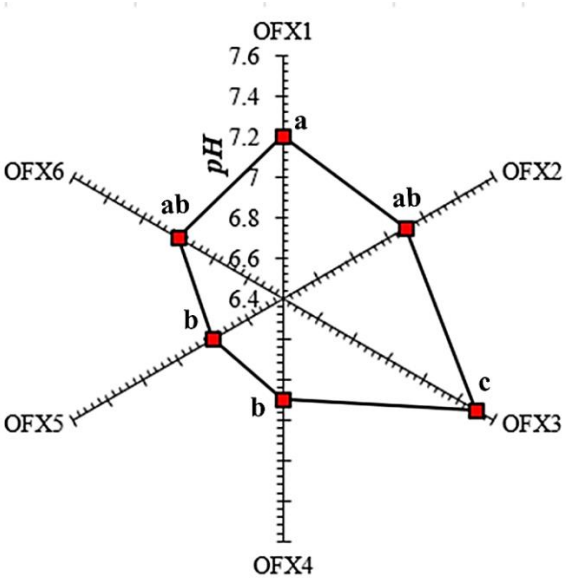

Fig. 5: The pH of different Ofloxacin-loaded nanoparticles containing *in situ* gel (OFX1-OFX6), Value not sharing a common letter differ significantly by one-way ANOVA (p<0.05, Tukey's test)

Only two formulations expressed significantly elevated pH than other formulations. While, OFX3 expressed significantly with a higher p-value (p<0.01, Tukey's test) with all the formulations, OFX1 expressed significantly higher pH (p<0.05, Tukey's test) with two formulations (OFX4, OFX5) with p-value lesser than that of OFX3.

Viscosity measurement

The viscosity of *in situ* gel formulations (OFX1-OFX6) reduced after exposure to simulated tear fluid. The viscosity of the some *in situ* formulations prepared using Poloxamer 407 decreased with increase in speed of the viscometer paddle irrespective of the presence of simulated tear fluid. Fascinatingly, *in situ* formulations prepared using Carbopol 943 (OFX4-OFX6) built up viscosity when the rotational speed of the viscometer was increased from 50 to 75 rpm. There was a decrease in viscosity beyond 75 rpm, with the least viscosity of the individual formulation at 100 rpm. The viscosity reduced significantly for the *in situ* formulations after contact with simulated tear fluid. The viscosities of *in situ* gel formulations (OFX1-OFX6) at different speeds is graphically illustrated in fig. 6.

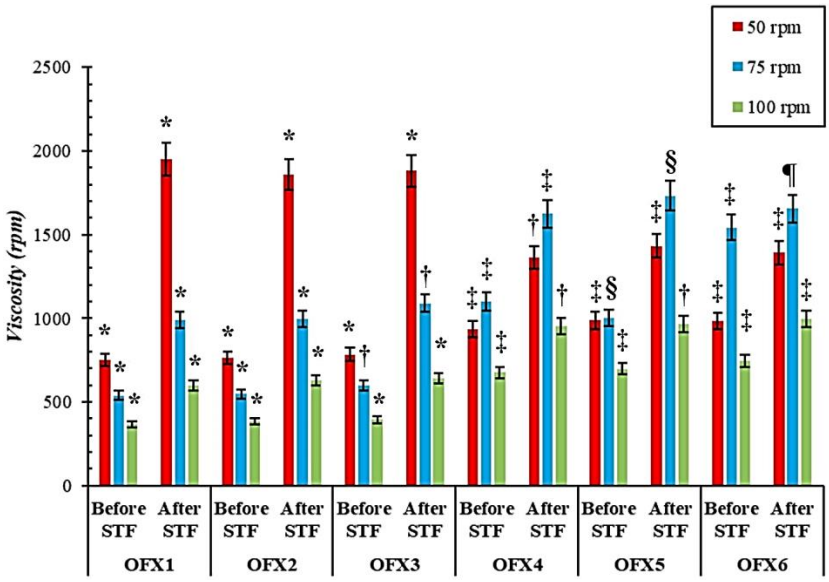

Fig. 6: Viscosities of different formulations (OFX1-OFX6) at different speeds before and after treatment with simulated tear fluid (STF), value with different symbols (e. g., *, ‡, §) at a given speed and condition (before or after STF) are significantly different (p < 0.05, Tukey's test)

Besides, there was significant difference in the viscosity with increase in viscometer speed (p<0.05) for each formulation. The formulations prepared using poloxamer-407 expressed significantly higher viscosity at 50 rpm (p<0.05, Tukey's test) and exhibited shear thinning effect with increase in viscometer speed. Interestingly, pseudoplastic flow behavior was demonstrated by the formulations prepared using Carbopol-943 after contact with STF. This behavior made the viscosities of these formulations (OFX4-OFX6) significantly higher (p<0.05, Tukey's test) than those containing poloxamer-407 (OFX1-OFX3) at 75 rpm after STF.

Determination of drug content

The drug content of ofloxacin in *in situ* gel formulations (OFX1-OFX6) was within the range of 96 to 99%, with the highest being OFX3 with 98.17%. The drug content of each formulation (OFX1-OFX6) is shown in table 3.

Table 3: Drug content of various *in situ* gel formulations (OFX1-OFX6)

Formulation code	Drug content
OFX1	96.66±0.16^{ab}
OFX2	97.25±0.23^{a}
OFX3	98.17±0.26^{c}
OFX4	96.69±0.27^{ab}
OFX5	96.22±0.19^{b}
OFX6	96.74±0.20^{ab}

Results are given as mean±SD (n=3). Formulations with same letters are not statistically different (p>0.05, Tukey's test). The drug content of OFX3 was significantly larger than other formulations (p<0.01, Tukey's test). OFX2 was only other formulation to show significantly higher (p<0.01, Tukey's test) drug content than at least one formulation (OFX5) other than OFX3.

***In vitro* diffusion studies**

All the formulations (OFX1-OFX6) released more than 90% at the end of 6 h (p<0.05), with OFX3 releasing 97.81%. It was interesting to note that OFX3 was the formulation exhibiting the highest immediate release of 35.63% after 30 min. The *in situ* gel prepared using poloxamer-407 expressed better immediate release (31-36%) compared to those containing Carbopol-943 (26-30%). The amount of drug release at the end of 6 h was also lesser in Carbopol 943 based *in situ* formulations (OFX4-OFX6: 90-93%) compared to poloxamer-407 *in situ* formulations (OFX1-OFX3: 94-98%). The drug release of OFX3 significantly differed (p<0.05, Tukey's test) from at least one of the formulations at all-time points except 0 h and 6 h point. The drug release of ofloxacin *in situ* gel containing the least concentration of Poloxamer 407 (OFX3) was significantly different from that containing the highest concentration of Carbopol 940 (OFX4) except the initial and final time points. The quantitative data of the release profiles of each formulation (OFX1-OFX6) are provided in *table 4*.

Even though, OFX3 and OFX4 expressed equivalent cumulative drug release to each other after 6 h, they expressed different drug release pattern which was statistically different (p<0.05, Tukey's test) at all points except initial and final timings (0 h and 6 h).

Table 4: *In vitro* dissolution release of ofloxacin-loaded nanoparticles containing *in situ* gels (OFX1-OFX6)

Time (h)	OFX1	OFX2	OFX3	OFX4	OFX5	OFX6
0	0.00±0.02^{a}	0.00±0.01^{a}	0.00±0.03^{a}	0.00±0.01^{a}	-0.01±0.01^{a}	0.00±0.01^{a}
0.5	31.32±2.04^{ab}	32.04±3.47^{ab}	35.63±3.78^{a}	26.15±3.42^{b}	28.76±2.50^{ab}	29.49±3.17^{ab}
1	43.53±4.21^{ab}	48.56±2.43^{a}	49.63±1.95^{a}	37.41±2.71^{b}	40.89±2.07^{b}	43.36±2.33^{ab}
2	50.19±2.93^{ab}	52.35±2.79^{ab}	56.52±3.02^{a}	45.98±3.62^{b}	50.14±1.89^{ab}	52.55±1.15^{ab}
3	64.96±2.67^{ab}	63.52±2.10^{ab}	68.31±3.77^{a}	58.09±3.59^{b}	62.32±1.62^{ab}	64.84±3.56^{ab}
4	73.14±3.02^{ab}	76.75±3.38^{a}	78.25±1.56^{a}	68.54±2.63^{b}	73.75±2.92^{ab}	74.39±2.35^{ab}
5	80.85±1.68^{ab}	88.54±3.77^{c}	89.78±3.32^{c}	79.36±3.64^{a}	86.09±4.87^{bc}	87.71±1.35^{bc}
6	93.92±3.55^{a}	96.26±2.85^{a}	97.81±2.56^{a}	90.67±2.61^{a}	92.16±2.55^{a}	93.05±3.02^{a}

Results are given as mean±SD (n=3). Formulations with same letters at a specific time point are not statistically different (p>0.05, Tukey's test).

The *in situ* formulations followed Higuchi model indicative of diffusion-controlled mechanism. Besides, Korsmeyer-Peppas model helped in understanding the diffusion mechanism of the formulations. The formulation followed Fickian diffusion being n-value less than 0.45 with linearity greater than 0.91. The Higuchi model expressed the highest slope range of 35 to 37. Nevertheless, a lowest slope was calculated in Hixson-Crowell model (-0.44 to-0.67). Based on the release kinetics of the of formulations, it was observed to strongly follow Higuchi model with excellent linearity ($0.981<R^2<0.996$). Besides, the release of the drug was observed to be highly dependent on remaining drug present in the nanoparticles-loaded *in situ* gel. Because, the first order kinetic models of all formulations expressed a linearities above 0.9 ($0.915<R^2<0.970$). Even though, OFX3 and OFX4 released more than 90% after 6 h, the high concentration of Carbopol made the drug release more independent compared to OFX3, which had the least concentration of poloxamer 407. This feature was observed as a higher linearity in zero order kinetics of OFX4 compared to OFX3. The linearity and slope under each kinetic model for all formulations (OFX1-OFX6) is tabulated in table 5.

Table 5: The kinetic profiles of different *in situ* gel formulations (OFX1-OFX6) containing slopes and linearities

Formulation	Zero order		First order		Higuchi		Hixson-crowell		Korsmeyer-peppas	
	R^2	Slope	R^2	Slope	R^2	Slope	R^2	Slope	R^2	Slope (n)
OFX1	0.900	13.015	0.918	-0.167	0.989	35.964	0.862	-0.535	0.968	0.380
OFX2	0.891	12.729	0.949	-0.208	0.982	35.081	0.961	-0.449	0.922	0.351
OFX3	0.880	13.598	0.965	-0.163	0.995	37.000	0.803	-0.667	0.969	0.342
OFX4	0.894	10.981	0.945	-0.148	0.992	35.473	0.878	-0.470	0.987	0.426
OFX5	0.896	14.058	0.966	-0.168	0.995	36.997	0.863	-0.505	0.988	0.414
OFX6	0.900	13.116	0.964	-0.176	0.982	36.404	0.868	-0.540	0.981	0.421

Initial 'burst' effect followed by sustained release was confirmed in the optimized batch OFX3. The initial 'burst' effect was confirmed by the rapid increase in the cumulative drug release more than 35%. Sustained release profile post initial 'burst' phase was confirmed by the Fickian diffusion mechanism (n<0.45).

Scanning electron microscopy (SEM)

The nanoparticles were observed to be in spherical or semi-spherical shape. The distribution of nanoparticles in the 1 µm level (*fig. 7(a)*) was uniform in nature. This states the effective loading of nanoparticles onto the *in situ* gel. In the 2µm resolution (*fig. 7(b)*), aggregation of nanoparticles was observed. This may be due to the drying process of the SEM procedure. It also helps us the recognize the polymeric matrix in which the nanoparticles are clumped together.

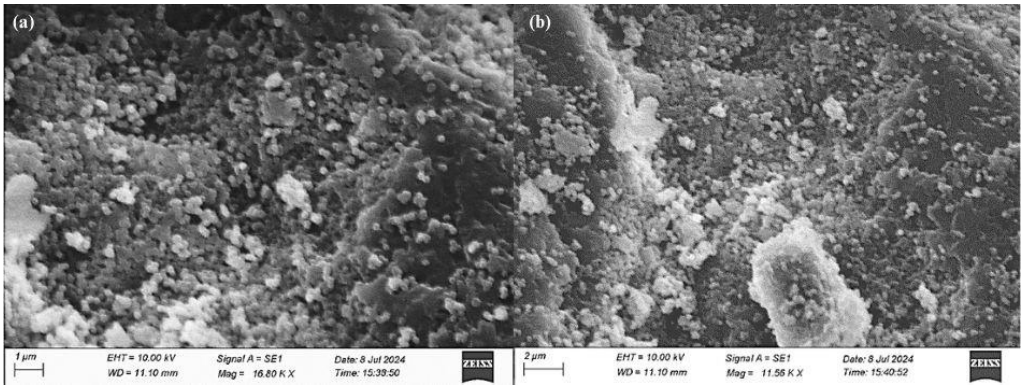

Fig. 7: Scanning electron microscopy image of optimized *in situ* gel formulation (OFX3) at magnification of (a) 1 µm and (b) 2 µm

In vitro HET-CAM test

A specific experiment called the HET-CAM test was conducted to investigate the imminence of the optimized formulation. Negative control (0.9% NaCl) demonstrated non-irritant in the form of normal tissue vascularization, while positive control (1% NaOH) demonstrated a moderate irritant that caused hemorrhage quicker than the negative control and optimized formulation (OFX3). There was no evidence of an inflammatory response in positive control and optimized formulation (OFX3). The irritancy score is shown in table 6.

Table 6: Irritancy score of different samples under *in vitro* HET-CAM assay

Name of sample	Haemorrhage time (sec)	Lysis time (sec)	Coagulation time (sec)	Irritancy score	Category
0.9% NaCl	300±0.57	295±1.00	290±0.57	0.48±0.01[a]	Non-irritant
OFX3	300±1.53	290±0.57	290±1.53	0.60±0.03[a]	Non-irritant
1% NaOH	210±1.00	180±1.53	150±1.53	8.87±0.01[b]	Moderate irritant

Results are given as mean±SD (n=3). The samples having same letters indicated significant difference ($p<0.05$, Tukey's test) between each other.

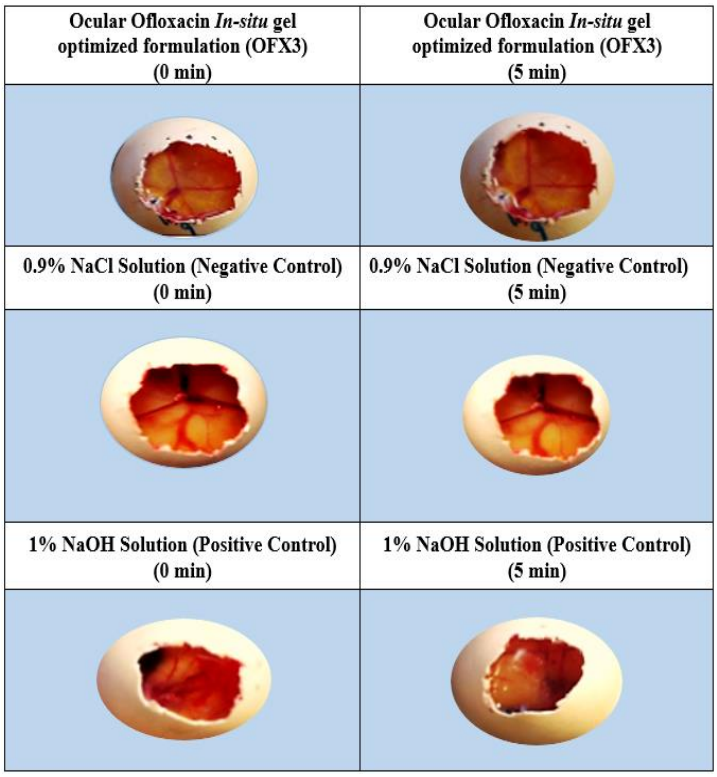

Fig. 8: Images of optimized formulation (OFX3) at 0 min and 5 min under *in vitro* HET-CAM assay

Stability studies

The stability of the optimized formulation (OFX3) was excellent since the selected formulation parameters were not showing significant changes even after 3 mo. The pH stayed within the acceptable limit range of 6.5 to 7.8. The viscosity of the optimized formulation was increased slightly after 3 mo, yet the

relative standard deviation (RSD) of the optimized formulation stayed within the acceptable range before and after STF (<±10%). irrespective of exposure to STF with no phase separation. However, drug content remained fairly constant during the period within the ICH Q1A (R2) limits (Assay: 90-110%). Drug release of the API was above 90% consistently throughout the experimental period (Drug release:>90% at 6 h). The stability parameters of the optimized formulation (OFX3) are tabulated in table 7.

Table 7: Stability parameters of optimized *in situ* gel formulation (OFX3)

Parameter			Initial	Mo-1	Mo-2	Mo-3
pH			7.5±0.13^{a}	7.6±0.03^{ab}	7.8±0.03^{b}	7.8±0.08^{b}
Viscosity	Before STF	50 rpm	1880.8±14.00^{a}	1892.7±10.72^{a}	1935.6±16.07^{a}	1998.4±12.42^{b}
(cps)		75 rpm	1090.8±30.45^{a}	1154.3±25.94^{b}	1133.5±25.11^{ab}	1132.8±22.75^{ab}
		100 rpm	640.4±25.58^{a}	654.2±25.16^{a}	655.9±22.50^{a}	680.3±28.40^{a}
	After STF	50 rpm	783.8±14.75^{a}	792.2±20.62^{a}	805.6±11.37^{a}	812.2±22.17^{a}
		75 rpm	600.3±11.50^{a}	625.5±9.71^{ab}	657.3±17.98^{b}	639.6±18.82^{ab}
		100 rpm	394.6±16.40^{a}	405.5±16.25^{a}	445.5±15.50^{b}	486.4±10.62^{b}
Assay (%)			98.17±0.26^{a}	98.67±0.13^{b}	98.34±0.20^{ab}	98.05±0.11^{a}
Drug release (%)			97.81±2.56^{a}	97.84±1.65^{a}	98.25±1.61^{a}	97.74±1.13^{a}

Results are given as mean±SD (n=3). The timepoints having same letters are not statistically different to each other within the row (p>0.05, Tukey's test). Besides, there was some statistically significant changes in the selected quantitative parameters over the stipulated period, however, stayed within the limit. Besides, the viscosity changed significantly (p<0.05, Tukey's test) irrespective of addition of STF throughout the experimental period.

DISCUSSION

Absorption maximum at 288 nm is an important peak for identification of Ofloxacin. *Nautiyal et al. (2012)* reported the content uniformity and *in vitro* diffusion of drug-loaded ocuserts at 288 nm [36]. Similarly, *Kośka et al. (2021)* developed an analytical technique for ofloxacin and ciprofloxacin by fixing the absorption maxima at 288 nm [37]. However, some research claims the absorption maxima (λ_{max}) to be in the range of 291-294 nm [38]. This hypsochromic shift for ofloxacin is observed due to the pH of the solvent employed for the analytical technique as a result of change in intensity of protonation effect [39]. The absorption maxima obtained for ethanol-water mixture (1:1) for ofloxacin (280 nm) was more hypsochromic than the result obtained (288 nm) in this research. Because, the ethanol in this research was used only for solubilization in small quantities. *Kaushal et al. (2023)*, on the other hand, utilized the solvents in equal proportions [40]. Increased acidity of methanol compared to water is an important reason for the shift. Hence, solvent pH plays a crucial role in UV spectrum of ofloxacin [41].

The carbonyl group (-C=O-) of ofloxacin was confirmed by the peak observed in the range between 1500 and 1700 cm^{-1}[42]. Besides, the C-F bond was confirmed by observing a peak in the range between 1000 and 1500 cm^{-1}[43]. The benzoxazine nucleus was confirmed by the presence of peaks observed in the range of 900 and 1200 cm^{-1}. These peaks are observed are due to presence of symmetric and anti-symmetric stretch of C-O-C, which can withstand not more than 200 °C [44].

Particle size distribution and zeta potential were analyzed for the ofloxacin-loaded nanoparticles before incorporation into *in situ* gel. Nanoparticle is generally defined as the structures which are ranging between 1 and 100 nm [45]. Nevertheless, there is no strict definition of particle size range since it can go up to a maximum of 1000 nm, as long as it stays within the nanoscopic size. In case of ocular delivery, the nanoparticles upto a maximum size of 1000 nm is considered [46]. Even though, smaller particle size offers improved surface area for absorption in the ocular cavity, it also possesses a drawback of quicker clearance from the conjunctiva. Larger particles tend to stay within the conjunctiva for a longer period, thereby effectively treating conjunctivitis [47]. Very large particles also are not recommended (≥ 2500 nm), because, it will be treated by ocular barriers as a foreign agent and will cause allergic reactions or rapidly eliminated [48]. The particle size and of the ofloxacin-loaded nanoparticles was equivalent to existing literature. *Li et al. (2018)* reported nanoparticles with mean size approximately 400 nm [49]. The drug-loaded NPs obtained in this research is much smaller than the mean particle size of nanocrystals of existing literature. The nanocrystals exhibited a particle size of>600 nm [50]. The particle size obtained in this research was similar to the emulsification-diffusion and salting out techniques [51]. Nanocrystals produced by *Baba et al. (2013)* were not uniformly size distributed since the standard deviation was in the range between 200 and 400 nm for fluorometholone and ranging between 400 and 900 nm for dexamethasone. This is usually due to changes in parameters during the process leading to inconsistent results. Sometimes, despite the uniform conditions of process, the particle aggregation tends to occur, leading to randomized particle size distribution. The results observed in the DLS failed to exhibit a polydispersity index below 0.3, which is due to the aggregation of particles observed in SEM at 2 µm (fig. 7(b)). This indicates that the process parameters must be further optimized to develop smaller nanoparticles with low polydispersity index (<0.3) than this research. [48, 52, 53]. Generally, chitosan-based nanoparticles greater than 100 nm are used for ocular delivery. *Sikhondze et al. (2023)* reported the sustained release of the medication from the formulation releasing more than 80% drug in 6 h. This is obtained as a result of large particle size distribution (500-1000 nm). It should be noted that pharmacological activity relies on ocular residence in *cul-de-sac* rather than permeation into deeper ocular tissues. [13, 14, 54] Polymers in the formulation interact with the nano particles in a charge-based mechanism. This influences the particle size of the nanoparticles incorporated in the formulation. These tend to neutralize the negative surface charge of the nanoparticles. This leads to adsorption of polymer on to the surface of nanoparticles. As a result, the hydrodynamic diameter of the particles is slightly increased in the formulation. [55, 56] *Abbas et al. (2022)* reported the increase in hydrodynamic size after dispersion into *in situ* gel. *Kesarla et al. (2016)* also reported an increase in particle size after incorporation into the *in situ* gel for ophthalmic purposes [24, 56].

Zeta potential helps in understanding the surface charge of the particles. Generally, the zeta potential with>±30mV indicates good stability, as a result of excellent electrostatic repulsion. As a result of electrostatic repulsion, there is minimal clumping or agglomeration of the particles within a sample [57, 58]. High zeta potential does not rule out the effect of agglomeration. This is due to the phenomenon of surface chemistry. Due to rough/irregular surfaces of particles, particle tends to adsorb with each other without forming bigger particles. This tends to shield the surface electric charge of the adsorbed particles [59]. When the surface of the particles is smooth and spherical in shape, Vanderwal's forces dominate over electrostatic forces. This is achieved by compression of electric double layer of particles which modifies the colloidal stability [60]. Sometimes, the zeta potential and PDI is not met sufficiently. PDI is generally high (>0.3) as a result of presence of traces of dust and debris. These tiny molecules drive up the strength of PDI through faster Brownian motion than nanoparticles [61]. Because, the

particle size distribution obtained in this research recognized only one sharp peak with high zeta potential. Hence, it is highly possible due to trace number of debris impacting PDI in spite of the high zeta potential [62]. The incorporation of nano particles in the *in situ* gel is not expected to increase the zeta potential towards neutralization. The shift in zeta potential observed in this research is plausible due to polymer adsorption onto the surface of nanoparticles. Similar trends have been reported for nanoparticle-laden ocular in situ gels and nanogel systems [24, 56].

The pH of formulations prepared using carbopol 943 were slightly acidic comparative to those prepared using poloxamer 407. This was consistent with recent literatures. The *in situ* prepared using poloxamer 407 by *Kurniawansyah et al.* (2020) (6.7-6.8) was slightly greater than those prepared using carbopol 934 by *Anbarasan et al.* (2019) (6.1-6.3) [63, 64]. This mild acidic condition of carbopol 943 based *in situ* gels is due to the protonating nature owing to multiple carboxylic acid groups. However, poloxamer 407 is neutral and non-ionic in nature and typically absent of acidic or basic functional groups [65].

Shear thinning effect was observed in *in situ* gels prepared using poloxamer-407 (OFX1-OFX3). This was due to reduction in viscosity with increase in speed of viscometer [66]. This non-Newtonian flow is common in *in situ* gels [67]. Fascinatingly, this pseudoplastic flow was not observed in *in situ* gels prepared using Carbopol 943 (OFX4-OFX6) up to a specific speed of viscometer. Beyond the point, the decrease in viscosity was observed similar to non-newtonian fluids [66, 68]. Formation of bulk network of carbomer molecules is an important reason for the initial shear thickening process. Gellan gum is crucial in increasing the viscosity of the *in situ* gel formulation [69, 70]. The *in situ* gel formulations exhibited low viscosity, which is suitable for ocular administration [71]. The increase in viscosity after exposure to simulated tear fluid indicates the formation of dense polymeric network within the ocular region, which is crucial for steady drug release [72]. An interestingly unusual feature of shear thickening was observed after simulated tear fluid contact. This is undesirable phenomenon observed in ocular *in situ* gels as it causes blurring vision due to buildup of viscosity covering the ocular region [73]. Dilute solutions with surfactant occasionally experience shear thickening effect as a result of micellization. Two or more micelles clump together to form a strong micellar network to resist initial shear. However, when the shear is further increased, the micellar network tends to break down developing a secondary shear thinning phase, which is a significant attribute for shear thickening liquids [74, 75].

Drug content of the ofloxacin ranged between 96% and 99%, which is consistent with recent literature. Our research reported a slightly greater drug content compared to *Prabhu et al.* [76] No formulation expressed a drug content more than 100% indicating the effective application of analytical procedure including proper cleaning to prevent trace drug in the instrument [77]. This ensures that the *in situ* gel was in sol form during the analytical procedure, because, gel form can cause inaccuracy in results, sometimes, giving results>100% [78].

The drug release for ocular products is often studied for 6 h, when compared to conventional of>8 h [79, 80]. Factors like lacrimation, blinking rate and nasolacrimal drainage govern the reduction of drug effect within the ocular cavities [81]. The drug release is not highly possible beyond 6 h in the case of conjunctivitis as a result of premature tear film break up [82]. The drug release of our *in situ* gel was sufficiently better than *Narayana et al. (2022)*. Although, the drug release expressed zero order kinetics similar to this research, it released up to a maximum of 80% after 6 h. This is obtained as a result of more sustained releasing nature of the *in situ* gel prepared by *Narayana et al. (2022)* [83]. It should be noted that sustained-release formulations must release adequate quantity of drug within the ocular cavities to ensure the therapeutic activity throughout the residence time of the formulation [84]. Initial burst of drug release, which was observed in this research, is an ideal strategy to release the maximum drug content within the ocular cavities under specified period. The drug concentration which is loosely encapsulated with nanoparticles and other free drug present in the *in situ* gel formulation dissolves rapidly as a result of high wettability. [85, 86] *Nayak et al. (2024)* expressed the formulations not showing the initial burst failed to release even 50% of the drug content *in vitro*. Hence, the initial burst observed in the formulations of our research played a pivotal role in the drug release>90% in 6 h [87]. Sustained release is mainly expressed in the presence of mucoadhesive network of the formulation prolonging the residence time with the ocular cavity [85]. The initial phase of burst effect is helpful in effectively treating the acute conditions of the ailment. On the other hand, sustained release phase aids in the prevention of troughs and peaks resulting in a drug concentration within the therapeutic window [88]. This biphasic nature is observed in nanoparticles-loaded *in situ* gels [89, 86].

The kinetic release of the *in situ* gels formulations (OFX1-OFX6) exhibited a diffusion-controlled mechanism [90]. This mechanism is related to the concentration gradient of the formulation [91]. Higuchi model was the closely fitted kinetic release model compared to other models. This release profile compares favorably with recent studies on thermogelling ocular gels. The drug release of carbopol-based *in situ* gels containing ofloxacin was observed to be>90% in the time range of 4.5 h to 6 h. This indicates the *in situ* gels performed in our research released>90% more uniformly at the 6 h point, attributing to a sustained release [92]. Hydrogel formulations containing ofloxacin exhibited more sustained release (75-80% at 9 h) than the current research. This phenomenon was possible, since it followed zero order kinetics. This was achieved by accomplishing dense crosslinked polymeric matrix. Besides, viscosity was enhanced by using HPMC in *Narayana et al.* (2022) [83]. Another research work of lomefloxacin *in situ* gel using poloxamer exhibited initial rapid release equivalent to the optimized formulation OFX3 in 30 min [93]. Following Higuchi model, optimized formulation (OFX3) mechanistically followed initial immediate release followed by the slow release occurs as a result of gelation property of poloxamer and Carbopol-based polymers [94]. This phenomenon is widely observed in ocular *in situ* gels. The sustained release is followed only after the *in situ* gel thickens increasing the residence time [95]. The drug release over time is inversely proportional to the concentration gradient since the drug concentration remaining within the formulation diminishes. This ultimately leads to the reduction in the driving force of the drug release process. Hence, it supports first order kinetics more than zero order kinetic model [96]. The drug release mechanism is quasi-fickian since the n-exponent is below 0.45 under Korsmeyer-Peppas model [97]. The Carbopol-943 *in situ* gels showed higher n-value than that of poloxamer [98, 99]. Quasi-Fickian release kinetics (n<0.45) with Higuchi Model as best fit observed in this study is evident in recent literature. Formulation of *in situ* gel Moxifloxacin-loaded nanoparticles exhibited fickian diffusion, which is water-rich channels allowing drug molecules to diffuse with minimal obstruction through temperature-triggered micellization and subsequent formation of a loosely crosslinked physical gel network [94, 100].

There was also an increase in linearity of zero order kinetics observed for *in situ* gels, when the concentration of poloxamer 407 was increased [101]. On the contrary, Carbopol concentration was inversely proportional to the linearity of zero order kinetics. High viscosity leads to restriction of drug diffusion and hence deviates from zero order kinetics [102]. The highest release of OFX3 was achieved due to an immediate outburst following first order kinetics. OFX4, on the other hand, failed to provide an equivalent immediate outburst of drug due to high carbopol concentration [103].

The spherical shape of the nanoparticles was visible in 1µm magnification at 16.80 kX (fig. 8 (a)). This shape was crucial to achieve maximum drug entrapment efficiency [104]. This was observed at a higher magnification in this research (16.80 kX) than *Kalaria et al. (2023)* (11.56 kX) [89]. Agglomeration or aggregation of nanoparticles was clearly visible at lower magnification (11.56 kX). Poloxamer-407 tends to form clumps rather than micelle-forming surfactant at high concentrations. However, it should be remembered that these surfactants, especially poloxamer-407, forms a polymeric matrix to promote sustained release of the API [104, 105]. This is in contrast with *Sharma et al. (2023)* since the

concentration of surfactant used is low concentration in the optimized formulation [104, 106]. Low concentrations of surfactant also fail to prevent agglomeration or aggregation of nanoparticles due to the steric hindrance between particles. However, 4% w/v is not a low concentration, since, narrow size distribution was observed [107]. Hence, hydrophobic interaction from the environment can cause a change in steric barrier and aggregate the nanoparticles. It was due to the high zeta potential of nanoparticles the shape and structure of nanoparticles stayed intact in the highest magnification of SEM [57, 108]. The process of agglomeration is responsible for the particle size distribution. This increases the polydispersity index due to the change in the existing particle size distribution [109]. Formulation processing parameters like mixing speed impact the particle size distribution and surface morphology of the nanoparticles. Hence, future directions of this research include optimization of the formulation processing parameters to prepare *in situ* gel with nanoparticles without undergoing agglomeration effect and possessing sufficiently low PDI (<0.3) [109, 110].

The *in vitro* HET-CAM assay is a widely adopted *ex-vivo* assay for understanding the ocular safety of the optimized formulation. The ethical approval of this assay is not mandatory with live animals not being used in this experimental setup [111]. Furthermore, the predictive power of this study is high because of the ability to detect coagulation and vessel lysis. The CAM is highly vascularized and closely resembles to healthy human conjunctival membrane [112]. The optimized formulation (OFX3) did not produce any hemorrhage and irritation. Isotonicity is maintained within the membrane even after the instillation of optimized formulation (OFX3) [111, 113].

Gatifloxacin *in situ* gel developed by *Kapoor et al. (2019)* also demonstrated a similar isotonic effect leading to the ocular safety of the formulation via healthy CAM. Sodium hydroxide is often employed as the negative control to understand the detrimental effects on CAM as it brings an isotonic imbalance. Besides, it causes coagulation via protein denaturation creating a highly alkaline environment caused in the instilled area [112, 114, 115].

CONCLUSION

Targeting the antibiotic within the ocular region is one of the significant challenges in pharmaceutical industry. The developed ofloxacin-loaded nanoparticulate *in situ* gel successfully integrates controlled release through prolonged ocular residence confirmed through diffusion-controlled matrix mechanism. The pH responsive drug release was successfully observed by gelation process under desired pH through electrostatic repulsion. The ability of administering this formulation as eye drops with reduced dosing frequency will enhance the patient compliance and adherence. With its promising *in vitro* performance, this formulation warrants further *in vivo* evaluation to consolidate its potential as a pioneering candidate for translational ophthalmic applications, ultimately benefiting patients with ocular infections. Future *in vivo* studies will further consolidate its potential as a pioneering candidate for translational ophthalmic applications.

ACKNOWLEDGEMENT

We would like to thank our principal of our college for providing immense support in completing our research. We would also extend our sincere thanks to PSG Institute of Advanced Studies and Annamalai University for conducting our evaluation studies.

FUNDING

None

AUTHORS CONTRIBUTIONS

Margret Chandira Rajappa-Conceptualization and approval of final draft; Gracy Gladin Solomon-Methodology, Writing initial draft; Nagasubramanian Venkatasubramaniam-Statistical Analysis, Data Interpretation, Reviewing and editing; Manoj Kumar Kumar-Data Collection; Dharshini Velmurugan-Methodology, Data Collection.

CONFLICT OF INTERESTS

Declared none

REFERENCES

1. Tesfahunegn Nigusse A, Tesfay Weldearegay K, Assefa Mezgebu H, Gebrehawarya Bisheu Y, Weldemhret Teweldemedhnt L, Hafte Amaha M. Conjunctivitis outbreak among children in central zone of Tigray, Northern Ethiopia 2023. JIEPH. 2024;7(4):52. doi: 10.37432/jieph.2024.7.4.143.
2. Gin C, Crock C, Wells K. Conjunctivitis: a review. Austr J Gen Pract. 2024 Nov 1;53(11):847-52. doi: 10.31128/ajgp-09-23-6960, PMID 39499843.
3. Chatterjee S, Gangwe AB, Agrawal D. Attack rates risk factors and productivity loss during an outbreak of acute conjunctivitis in central India. J Clin Ophthalmol Res. 2025 Jul 1;13(3):286-94. doi: 10.4103/jcor.jcor_47_25.
4. Azari AA, Barney NP. Conjunctivitis: a systematic review of diagnosis and treatment. JAMA. 2013 Oct 22;310(16):1721-9. doi: 10.1001/jama.2013.280318, PMID 24150468.
5. Seitzman GD, Prajna L, Prajna NV, Sansanayudh W, Satitpitakul V, Laovirojjanakul W. Biomarker detection and validation for corneal involvement in patients with acute infectious conjunctivitis. JAMA Ophthalmol. 2024 Aug 15;142(9):865-71. doi: 10.1001/jamaophthalmol.2024.2891, PMID 39145969.
6. Kareem Rhumaid A, Alak Mahdi Al-Buhilal J, Al-Rubaey NK, Yassen Al-Zamily K. Prevalence and antibiotic susceptibility of pathogenic bacteria associated with ocular infections in adult patients. Arch Razi Inst. 2022 Oct 1;77(5):1917-24. doi: 10.22092/ARI.2022.359510.2437, PMID 37123163.
7. Singh S, Oberoi L, Singh K, Malhotra A, Soneja S, Singh K. Microbiological spectrum of ocular infections in patients of Tertiary Care Eye Hospital of Punjab. IJMMTD. 2021;7(3):154-9. doi: 10.18231/j.ijmmtd.2021.033.
8. Vatlin AA, Bekker OB, Shur KV, Ilyasov RA, Shatrov PA, Maslov DA. Kanamycin and ofloxacin activate the intrinsic resistance to multiple antibiotics in Mycobacterium smegmatis. Biology. 2023 Mar 27;12(4):506. doi: 10.3390/biology12040506, PMID 37106707.
9. Drago L, Minasi V, Lembo A, Uslenghi A, Benedetti S, Covi M. Antibiotic resistance profiles in eye infections: a local concern with a retrospective focus on a large hospital in Northern Italy. Microorganisms. 2024 May 14;12(5):984. doi: 10.3390/microorganisms12050984, PMID 38792813.
10. Dosmar E, Walsh J, Doyel M, Bussett K, Oladipupo A, Amer S. Targeting ocular drug delivery: an examination of local anatomy and current approaches. Bioengineering (Basel). 2022 Jan 17;9(1):41. doi: 10.3390/bioengineering9010041, PMID 35049750.
11. Han H, Li S, Xu M, Zhong Y, Fan W, Xu J. Polymer and lipid-based nanocarriers for ocular drug delivery: current status and future perspectives. Adv Drug Deliv Rev. 2023 Mar 7;196:114770. doi: 10.1016/j.addr.2023.114770, PMID 36894134.
12. Beal C, Giordano B. Clinical evaluation of red eyes in pediatric patients. J Pediatr Health Care. 2016 Mar 2;30(5):506-14. doi: 10.1016/j.pedhc.2016.02.001, PMID 26948259.
13. Vo A, Feng X, Patel D, Mohammad A, Kozak D, Choi S. Factors affecting the particle size distribution and rheology of brinzolamide ophthalmic suspensions. Int J Pharm. 2020 Jun 14;586:119495. doi: 10.1016/j.ijpharm.2020.119495, PMID 32553495.
14. Motwani SK, Chopra S, Talegaonkar S, Kohli K, Ahmad FJ, Khar RK. Chitosan–sodium alginate nanoparticles as submicroscopic reservoirs for ocular delivery: formulation optimisation and *in vitro* characterisation. Eur J Pharm Biopharm. 2007 Sep 25;68(3):513-25. doi: 10.1016/j.ejpb.2007.09.009, PMID 17983737.
15. Kumar D, Jain N, Gulati N, Nagaich U. Nanoparticles laden in situ gelling system for ocular drug targeting. J Adv Pharm Technol Res. 2013 Jan 1;4(1):9-17. doi: 10.4103/2231-4040.107495, PMID 23662277.

16. Bisen AC, Dubey A, Agrawal S, Biswas A, Rawat KS, Srivastava S. Recent updates on ocular disease management with ophthalmic ointments. Ther Deliv. 2024 Jun 2;15(6):463-80. doi: 10.1080/20415990.2024.2346047, PMID 38888757.
17. Yang Y, Lockwood A. Topical ocular drug delivery systems: innovations for an unmet need. Exp Eye Res. 2022 Mar 4;218:109006. doi: 10.1016/j.exer.2022.109006, PMID 35248559.
18. Tapply I, Broadway DC. Improving adherence to topical medication in patients with glaucoma. Patient Prefer Adherence. 2021 Jul 1;15:1477-89. doi: 10.2147/PPA.S264926, PMID 34239297.
19. Nair AB, Shah J, Jacob S, Al-Dhubiab BE, Sreeharsha N, Morsy MA. Experimental design formulation and *in vivo* evaluation of a novel topical in situ gel system to treat ocular infections. PLOS One. 2021 Mar 19;16(3):e0248857. doi: 10.1371/journal.pone.0248857, PMID 33739996.
20. Singh A, Rajora A, Mazumder R, Padhi S. Effect of Zein on ciprofloxacin floating tablets. Int J App Pharm. 2022 Nov 7;14(6):137-47. doi: 10.22159/ijap.2022v14i6.45354.
21. Suresh A, Gonde S, Mondal PK, Sahoo J, Chopra D. Improving solubility and intrinsic dissolution rate of ofloxacin API through salt formation via mechanochemical synthesis with diphenic acid. J Mol Struct. 2020 Jul 2;1221:128806. doi: 10.1016/j.molstruc.2020.128806.
22. Mushtaq K, Saeed M, Gul W, Munir M, Firdous A, Yousaf T. Synthesis and characterization of TiO_2 via sol-gel method for efficient photocatalytic degradation of antibiotic ofloxacin. Inorg Nano-Met Chem. 2020 Feb 17;50(7):580-6. doi: 10.1080/24701556.2020.1722695.
23. Rajappa MC, Kannan A, Venkatasubramaniam N, Venkatachalam L, Karnan S, Antonysamy D. Improved wound healing activity through synergistic approach of pumpkin seed oil and curcumin loaded model in microgel. Int J App Pharm. 2025 Sep 7;18(4):238-52. doi: 10.22159/ijap.2025v17i5.54322.
24. Kesarla R, Tank T, Vora PA, Shah T, Parmar S, Omri A. Preparation and evaluation of nanoparticles loaded ophthalmic in situ gel. Drug Deliv. 2015 Jan 12;23(7):2363-70. doi: 10.3109/10717544.2014.987333, PMID 25579467.
25. Paradkar MU, Parmar M. Formulation development and evaluation of Natamycin niosomal in-situ gel for ophthalmic drug delivery. J Drug Deliv Sci Technol. 2017 Mar 7;39:113-22. doi: 10.1016/j.jddst.2017.03.005.
26. El-Emam GA, Motawea A, El Hady WE, Saber S, Mourad AA, Ramadan HA. Salutary influence of gemifloxacin mesylate nanocubosomes based-in situ ocular gel as a novel approach for the management of experimental keratitis induced by MRSA. J Drug Deliv Sci Technol. 2023 Oct 9;89:105012. doi: 10.1016/j.jddst.2023.105012.
27. Datta S, Bhowmik R, Nath R, Chakraborty R, Chakraborty A. Formulation and evaluation of a nanoparticle laden in situ gel system for enhancing the ocular delivery of ciprofloxacin. IJPSRR. 2021 Oct 15;70(2):156-63. doi: 10.47583/ijpsrr.2021.v70i02.018.
28. Wadhwa K, Sharma C, Goswami M, Thakur N. Formulation and evaluation of pH triggered in situ ocular gel of ofloxacin. Int J Pharm Sci Res. 2019 Oct 1;10(10):4507-12. doi: 10.13040/ijpsr.0975-8232.10(10).4507-12.
29. Gupta C, Juyal V, Nagaich U. Formulation optimization and evaluation of in situ gel of moxifloxacin hydrochloride for ophthalmic drug delivery. Int J App Pharm. 2019 Mar 6;11(4):147-58. doi: 10.22159/ijap.2019v11i4.30388.
30. Jagdale S, Shewale N, Kuchekar BS. Optimization of thermoreversible in situ nasal gel of timolol maleate. Scientifica. 2016 Jan 1;2016:6401267. doi: 10.1155/2016/6401267, PMID 27293975.
31. Chandira RM, Pethappachetty P, Venkatasubramaniam N, Antony Samy DA. Formulation and comparison of glucomannan metallocomplexes made of cobalt and copper. Asian J Biol Life Sci. 2022 Sep 20;11(2):564-9. doi: 10.5530/ajbls.2022.11.76.
32. Ondieki ASK, Rathore KS. Development and characterization of topical gel containing deep eutectic mixture of luliconazole for topical drug delivery system. Int J Pharm Chem Anal. 2023;10(4):294-302. doi: 10.18231/j.ijpca.2023.049.
33. Maddiboyina B, Jhawat V, Desu PK, Gandhi S, Nakkala RK, Singh S. Formulation and evaluation of thermosensitive flurbiprofen in situ nano gel for the ocular delivery. J Biomater Sci Polym Ed. 2021 May 12;32(12):1584-97. doi: 10.1080/09205063.2021.1927460, PMID 33977874.
34. Balu A, Johnson T, Sundara R, Seetharaman S. Optimization and evaluation of temperature triggered in situ gel formulation using design of experiments (DoE) and HET-CAM test. J Nanomed. 2020 Dec 9;3(1):1031. doi: 10.15520/jnm.v3i1.1031.
35. Vijaya Rani KR, Rajan S, Bhupathyraaj M, Priya RK, Halligudi N, Al-Ghazali MA. The effect of polymers on drug release kinetics in nanoemulsion in situ gel formulation. Polymers. 2022 Jan 21;14(3):427. doi: 10.3390/polym14030427, PMID 35160417.
36. Nautiyal D, Singh V, Ali S. Formulation and evaluation of sustained release of ofloxacin ocular inserts. Res J Pharm Technol. 2012 Dec;5(12):1497-9. doi: 10.52711/0974-360X.
37. Koska I, Purgat K, Glowacki R, Kubalczyk P. Simultaneous determination of ciprofloxacin and ofloxacin in animal tissues with the use of capillary electrophoresis with transient pseudo-isotachophoresis. Molecules. 2021 Nov 17;26(22):6931. doi: 10.3390/molecules26226931, PMID 34834024.
38. Meghna S, Usman S, Kumar CD, Thangabalan B. A review on reported analytical methods for estimation of ofloxacin. Int J Pharm Sci. 2025;3(5):734-65. doi: 10.5281/zenodo.15341908.
39. Qin Y, Qin J, Zhou X, Yang Y, Chen R, Tan J. Effects of pH on light absorption properties of water-soluble organic compounds in particulate matter emitted from typical emission sources. J Hazard Mater. 2021 Nov 3;424(C):127688. doi: 10.1016/j.jhazmat.2021.127688, PMID 34775306.
40. Kaushal P, Kumar Kushawaha S, Majumder M, Singh Ashawat M. Validated analytical method for multicomponent analysis of famotidine and ofloxacin in bulk drug and tablet formulation by using UV-visible spectrophotometer and RP-HPLC. Asian J Pharm Anal. 2023 Sep 7;13(3):162-70. doi: 10.52711/2231-5675.2023.00026.
41. Abrash HI. The relative acidities of water and methanol. J Chem Educ. 2001 Nov 1;78(11):1496. doi: 10.1021/ed078p1496.
42. Khan A, Andleeb A, Azam M, Tehseen S, Mehmood A, Yar M. Aloe vera and ofloxacin incorporated chitosan hydrogels show antibacterial activity stimulate angiogenesis and accelerate wound healing in full thickness rat model. J Biomed Mater Res B Appl Biomater. 2022 Sep 2;111(2):331-42. doi: 10.1002/jbm.b.35153, PMID 36053925.
43. Jha KK, Jha AK. Synthesis and spectral characterization of fluoroquinolone-ofloxacin. Int J Chem Stud. 2020 Jan 1;4(4):1-3.
44. Ohashi S, Cassidy F, Huang S, Chiou K, Ishida H. Synthesis and ring-opening polymerization of 2-substituted 1,3-benzoxazine: the first observation of the polymerization of oxazine ring-substituted benzoxazines. Polym Chem. 2016 Jan 1;7(46):7177-84. doi: 10.1039/c6py01686c.
45. Datta D, Priyanka Bandi S, Colaco V, Dhas N, Siva Reddy DV, Vora LK. Fostering the unleashing potential of nanocarriers-mediated delivery of ocular therapeutics. Int J Pharm. 2024;658:124192. doi: 10.1016/j.ijpharm.2024.124192, PMID 38703931.
46. Hadinoto K, Sundaresan A, Cheow WS. Lipid–polymer hybrid nanoparticles as a new generation therapeutic delivery platform: a review. Eur J Pharm Biopharm. 2013 Jul 17;85(3 Pt A):427-43. doi: 10.1016/j.ejpb.2013.07.002, PMID 23872180.
47. Mok ZH. The effect of particle size on drug bioavailability in various parts of the body. Pharm Sci Adv. 2023 Nov 23;2:100031. doi: 10.1016/j.pscia.2023.100031, PMID 41550144.
48. Grassiri B, Zambito Y, Bernkop Schnurch A. Strategies to prolong the residence time of drug delivery systems on ocular surface. Adv Colloid Interface Sci. 2020 Dec 13;288:102342. doi: 10.1016/j.cis.2020.102342, PMID 33444845.
49. Li J, Tian S, Tao Q, Zhao Y, Gui R, Yang F. Montmorillonite/chitosan nanoparticles as a novel controlled-release topical ophthalmic delivery system for the treatment of glaucoma. Int J Nanomedicine. 2018 Jul 10;13:3975-87. doi: 10.2147/IJN.S162306, PMID 30022821.

50. Baba K, Nishida K. Steroid nanocrystals prepared using the nano spray dryer B-90. Pharmaceutics. 2013 Jan 25;5(1):107-14. doi: 10.3390/pharmaceutics5010107, PMID 24300400.
51. Gorantla S, Rapalli VK, Waghule T, Singh PP, Dubey SK, Saha RN. Nanocarriers for ocular drug delivery: current status and translational opportunity. RSC Adv. 2020 Jan 1;10(46):27835-55. doi: 10.1039/d0ra04971a, PMID 35516960.
52. Mota WS, Severino P, Kadian V, Rao R, Zielinska A, Silva AM. Nanometrology: particle sizing and influence on the toxicological profile. Front Nanotechnol. 2025 May 6;7:1559523. doi: 389/fnano.2025.1479464.
53. Masarudin MJ, Cutts SM, Evison BJ, Phillips DR, Pigram PJ. Factors determining the stability size distribution and cellular accumulation of small monodisperse chitosan nanoparticles as candidate vectors for anticancer drug delivery: application to the passive encapsulation of ^{14}C-doxorubicin. Nanotechnol Sci Appl. 2015 Dec 11;8:67-80. doi: 10.2147/NSA.S91785, PMID 26715842.
54. Sikhondze SS, Makoni PA, Walker RB, Khamanga SM. Chitosan-coated sln: a potential system for ocular delivery of metronidazole. Pharmaceutics. 2023 Jun 30;15(7):1855. doi: 10.3390/pharmaceutics15071855, PMID 37514041.
55. Pham DT, Navesit K, Wiwatkunupakarn L, Chomchalao P, Tiyaboonchai W. Nanoparticles-hydrogel composites: a promising innovative system for local antimicrobial applications. J Drug Deliv Sci Technol. 2023 Oct 10;89:105055. doi: 10.1016/j.jddst.2023.105055.
56. Abbas MN, Khan SA, Sadozai SK, Khalil IA, Anter A, Fouly ME. Nanoparticles loaded thermoresponsive in situ gel for ocular antibiotic delivery against bacterial keratitis. Polymers. 2022 Mar 11;14(6):1135. doi: 10.3390/polym14061135, PMID 35335465.
57. Ozturk K, Kaplan M, Calıs S. Effects of nanoparticle size shape and zeta potential on drug delivery. Int J Pharm. 2024 Oct 1;666:124799. doi: 10.1016/j.ijpharm.2024.124799, PMID 39369767.
58. Salamah M, Sipos B, Schelz Z, Zupko I, Kiricsi A, Szalenko Tokes A. Development *in vitro* and ex vivo characterization of lamotrigine-loaded bovine serum albumin nanoparticles using QbD approach. Drug Deliv. 2025 Feb 3;32(1):2460693. doi: 10.1080/10717544.2025.2460693, PMID 39901331.
59. Zaman M, Ahmad E, Qadeer A, Rabbani G, Khan RH. Nanoparticles in relation to peptide and protein aggregation. Int J Nanomedicine. 2014 Feb 1;9:899-912. doi: 10.2147/IJN.S54171, PMID 24611007.
60. Johnson L, Gray DM, Niezabitowska E, McDonald TO. Multi-stimuli-responsive aggregation of nanoparticles driven by the manipulation of colloidal stability. Nanoscale. 2021 Jan 1;13(17):7879-96. doi: 10.1039/d1nr01190a, PMID 33881098.
61. Rodriguez-Loya J, Lerma M, Rodriguez-Loya JL. Dynamic light scattering and its application to control nanoparticle aggregation in colloidal systems: a review. Micromachines. 2023 Dec 22;15(1):24. doi: 10.3390/mi15010024, PMID 38258143.
62. Farkas N, Kramar JA. Dynamic light scattering distributions by any means. J Nanopart Res. 2021 May 1;23(5):120. doi: 10.1007/s11051-021-05220-6, PMID 39381776.
63. Kurniawansyah IS, Rusdiana T, Sopyan I, Ramoko H, Wahab HA, Subarnas A. In situ ophthalmic gel forming systems of poloxamer 407 and hydroxypropyl methyl cellulose mixtures for sustained ocular delivery of chloramphenicole: optimization study by factorial design. Heliyon. 2020 Nov 1;6(11):e05365. doi: 10.1016/j.heliyon.2020.e05365, PMID 33251348.
64. Anbarasan B, Kumar RS, Thanka J, Ramaprabhu S, Shanmuganathan S. Preparation and characterization of pH based carbopol 934P in situ hydrogels for the treatment of harmful bacterial infections. Int J Pharm Sci Res. 2019 Jan 1;10(1):232-44. doi: 10.13040/ijpsr.0975-8232.10(1).232-44.
65. Wu Y, Liu Y, Li X, Kebebe D, Zhang B, Ren J. Research progress of in-situ gelling ophthalmic drug delivery system. Asian J Pharm Sci. 2018 May 24;14(1):1-15. doi: 10.1016/j.ajps.2018.04.008, PMID 32104434.
66. Chiodza K, Goosen NJ. Viscosity mixing regime and power consumption analysis during enzymatic hydrolysis of fish (Sardina pilchardus) processing by-products through development of power number and Reynolds number correlations. Food Bioprod Process. 2024;143:178-90. doi: 10.1016/j.fbp.2023.11.008.
67. Brahmavale M. From liquid to solid: unravelling the magic of in situ gels. IJRASET. 2024 May 23;12(5):3829-37. doi: 10.22214/ijraset.2024.62471.
68. Harish NM, Prabhu P, Charyulu RN, Gulzar MA, Subrahmanyam EV. Formulation and evaluation of in situ gels containing clotrimazole for oral candidiasis. Indian J Pharm Sci. 2009 Jul;71(4):421-7. doi: 10.4103/0250-474X.57291, PMID 20502548.
69. Maslii Y, Ruban O, Kasparaviciene G, Kalveniene Z, Materiienko A, Ivanauskas L. The influence of pH values on the rheological textural and release properties of carbomer Polacril® 40P-based dental gel formulation with plant-derived and synthetic active components. Molecules. 2020 Oct 29;25(21):5018. doi: 10.3390/molecules25215018, PMID 33138200.
70. Sulaiman HT, Jabir SA, Kadhem Al-kinani K. Investigating the effect of different grades and concentrations of PH-sensitive polymer on preparation and characterization of lidocaine hydrochloride as in situ gel buccal spray. Asian J Pharm Clin Res. 2018;11(11):401. doi: 10.22159/ajpcr.2018.v11i11.28492.
71. Kolawole OM, Cook MT. In situ gelling drug delivery systems for topical drug delivery. Eur J Pharm Biopharm. 2023 Jan 13;184:36-49. doi: 10.1016/j.ejpb.2023.01.007, PMID 36642283.
72. Chowhan A, Ghosh B, Giri TK. Composite ion responsive in situ gel based on Gellan/carboxymethyl cellulose blend for improved gelation and sustained acyclovir ocular release. Ind J Pharm Sci. 2023 Jan 1;85(3):581-91. doi: 10.36468/pharmaceutical-sciences.1125.
73. Terreni E, Zucchetti E, Tampucci S, Burgalassi S, Monti D, Chetoni P. Combination of nanomicellar technology and in situ gelling polymer as ocular drug delivery system (ODDS) for cyclosporine-a. Pharmaceutics. 2021 Feb 1;13(2):192. doi: 10.3390/pharmaceutics13020192, PMID 33535607.
74. Barentin C, Liu AJ. Shear thickening in dilute solutions of wormlike micelles. Europhys Lett. 2001 Aug 1;55(3):432-8. doi: 10.1209/epl/i2001-00432-x.
75. Serra GF, Oliveira L, Gurgen S, De Sousa RJ, Fernandes FA. Shear thickening fluid (STF) in engineering applications and the potential of cork in STF-based composites. Adv Colloid Interface Sci. 2024;327:103157. doi: 10.1016/j.cis.2024.103157, PMID 38626554.
76. Prabhu A, Koland M. Development and evaluation of an in situ thermogelling system of ofloxacin for controlled ocular delivery. Asian J Pharm Clin Res. 2019 Mar;12(3):567-70. doi: 10.22159/ajpcr.2019.v12i3.31233.
77. Kim BH, Lee W, Kim YL, Lee JH, Hong J. Efficient matrix cleanup of soft-gel-type dietary supplements for rapid screening of 92 illegal adulterants using EMR-lipid dSPE and UHPLC-Q/TOF-MS. Pharmaceuticals (Basel). 2021 Jun 15;14(6):570. doi: 10.3390/ph14060570, PMID 34203614.
78. Peterfi O, Meszaros LA, Szabo Szocs B, Ficzere M, Sipos E, Farkas A. UV-vis imaging-based investigation of API concentration fluctuation caused by the sticking behaviour of pharmaceutical powder blends. Int J Pharm. 2024 Mar 15;655:124010. doi: 10.1016/j.ijpharm.2024.124010, PMID 38493839.
79. Khan FU, Nasir F, Iqbal Z, Neau S, Khan I, Hassan M. Improved ocular bioavailability of moxifloxacin HCl using PLGA nanoparticles: fabrication characterization *in vitro* and *in vivo* evaluation. Iran J Pharm Res. 2021 Jan 1;20(3):592-608. doi: 10.22037/ijpr.2021.114478.15054, PMID 34904011.
80. Raut R, Deore R, Patil S, Pachorkar S, Mungse V. Sustained release drug delivery system: a review. Int J Pharm Res Appl. 2021 Jul;6(4):953-66. doi: 10.35629/7781-0604953966.
81. Shen J, Lu GW, Hughes P. Targeted ocular drug delivery with pharmacokinetic/pharmacodynamic considerations. Pharm Res. 2018 Sep 25;35(11):217. doi: 10.1007/s11095-018-2498-y, PMID 30255364.
82. Khurana AK, Moudgil SS, Parmar IP, Ahluwalia BK. Tear film flow and stability in acute and chronic conjunctivitis. Acta

Ophthalmol (Copenh). 1987 Jun;65(3):303-5. doi: 10.1111/j.1755-3768.1987.tb08510.x, PMID 3618153.
83. Narayana S, Ahmed MG. Design and evaluation of ocular hydrogel containing combination of ofloxacin and dexamethasone for the treatment of conjunctivitis. Braz J Pharm Sci. 2022 Jan 1;58:e20180. doi: 10.1590/s2175-97902022e20180.
84. Drago L. Topical antibiotic therapy in the ocular environment: the benefits of using moxifloxacin eyedrops. Microorganisms. 2024 Mar 25;12(4):649. doi: 10.3390/microorganisms12040649, PMID 38674593.
85. Desai N, Colley HE, Krishna Y, Bosworth LA, Kearns VR. Mucoadhesive nanofibers for ocular drug delivery: mechanisms design strategies and applications. Drug Deliv Transl Res. 2025 Jun 25;15(6):1-40. doi: 10.1007/s13346-025-01894-w, PMID 40562965.
86. Herdiana Y, Wathoni N, Shamsuddin S, Muchtaridi M. Drug release study of the chitosan-based nanoparticles. Heliyon. 2021 Dec 24;8(1):e08674. doi: 10.1016/j.heliyon.2021.e08674, PMID 35028457.
87. Nayak D, Kondepati HV, Rathnanand M, Tippavajhala VK. Statistical optimization and evaluation of in situ gel for the ocular delivery of cromolyn sodium. Int J App Pharm. 2024 Mar 7;16(2):124-31. doi: 10.22159/ijap.2024v16i2.49781.
88. Cam ME, Yildiz S, Alenezi H, Cesur S, Ozcan GS, Erdemir G. Evaluation of burst release and sustained release of pioglitazone-loaded fibrous mats on diabetic wound healing: an *in vitro* and *in vivo* comparison study. J R Soc Interface. 2020 Jan 1;17(162):20190712. doi: 10.1098/rsif.2019.0712, PMID 31964272.
89. Kalaria VJ, Saisivam S, Alshishani A, Aljariri Alhesan JS, Chakraborty S, Rahamathulla M. Design and evaluation of in situ gel eye drops containing nanoparticles of gemifloxacin mesylate. Drug Deliv. 2023 Dec;30(1):2185180. doi: 10.1080/10717544.2023.2185180, PMID 36876464.
90. Jalwal P, Deepak, Shailja J, Ajit, Gourav SG, Sardana S. Formulation and characterization of ofloxacin-loaded nanoparticles. J Pharm Innov J. 2017;7(8):615-7.
91. Fu Y, Kao WJ. Drug release kinetics and transport mechanisms of non-degradable and degradable polymeric delivery systems. Expert Opin Drug Deliv. 2010 Apr;7(4):429-44. doi: 10.1517/17425241003602259, PMID 20331353.
92. Murthy GL, Kumar VG, Sravani B, Kumar SS, Kumar DA, Prasad AB, Sri B, Prasanna DDGL, Prasad MR, Prasad RS. Design and development of ofloxacin insitu gel using mucoadhesive polymers. Sch Acad J Pharmacol. 2017;6(5):212-20. doi: 10.21276/sajp.
93. Gadad AP, Wadklar PD, Dandghi P, Patil A. Thermosensitive in situ gel for ocular delivery of lomefloxacin. Ind J Pharm Edu Res. 2015;50(2s):S96-S105. doi: 10.5530/ijper.50.2.24.
94. Gurav NH, Husukale PS. Development and evaluation of in situ gel formation for treatment of mouth ulcer. Turk J Pharm Sci. 2023;20(3):185-97. doi: 10.4274/tjps.galenos.2022.25968, PMID 37417201.
95. Shreya L, Suma US, Zohmingliani R. Recent advances in oral in situ gel drug delivery system: a polymeric approach. Drug Dev Ind Pharm. 2025 Sep 8;51(12):1639-49. doi: 10.1080/03639045.2025.2559033, PMID 40920034.
96. Adepu S, Ramakrishna S. Controlled drug delivery systems: current status and future directions. Molecules. 2021 Sep 29;26(19):5905. doi: 10.3390/molecules26195905, PMID 34641447.
97. Ahmed L, Atif R, Eldeen TS, Yahya I, Omara A, Eltayab M. Study the using of nanoparticles as drug delivery system based on mathematical models for controlled release. Int J Latest Technol Eng Manag Appl Sci. 2019;8(5):52-6.
98. Costa P, Sousa Lobo JM. Modeling and comparison of dissolution profiles. Eur J Pharm Sci. 2001 May 1;13(2):123-33. doi: 10.1016/s0928-0987(01)00095-1, PMID 11297896.
99. Sheshala R, Ming NJ, Kok YY, Raj Singh TR, Dua K. formulation and characterization of ph induced in situ gels containing sulfacetamide sodium for ocular drug delivery: a combination of carbopol®/ HPMC polymer. Ind J Pharm Educ Res. 2019 Sep 25;53(4):654-62. doi: 10.5530/ijper.53.4.127.
100. Upadhyay Shivam U, Chavan Siddhi K, Gajjar Devarshi U, Upadhyay Umeshkumar M, Jayvadan KP. Nanoparticles laden in situ gel for sustained drug release after topical ocular administration. J Drug Deliv Sci Technol. 2020;57:101736. doi: 10.1016/j.jddst.2020.101736.
101. Mod Razif MR, Chan SY, Widodo RT, Chew YL, Hassan M, Hisham SA. Optimization of a luteolin-loaded TPGS/poloxamer 407 nanomicelle: the effects of copolymers hydration temperature and duration and freezing temperature on encapsulation efficiency particle size and solubility. Cancers (Basel). 2023 Jul 24;15(14):3741. doi: 10.3390/cancers15143741, PMID 37509402.
102. Suhail M, Wu PC, Minhas MU. Using carbomer-based hydrogels for control the release rate of diclofenac sodium: preparation and *in vitro* evaluation. Pharmaceuticals (Basel). 2020 Nov 17;13(11):399. doi: 10.3390/ph13110399, PMID 33212866.
103. Laracuente ML, Yu MH, McHugh KJ. Zero-order drug delivery: state of the art and future prospects. J Control Release. 2020 Sep 12;327:834-56. doi: 10.1016/j.jconrel.2020.09.020, PMID 32931897.
104. Sharma A, Sharma S, Tomar DS. Optimization of in-situ nanoparticulate gel of ofloxacin using factorial design to improve treatment strategy for conjunctivitis and corneal ulcers. Ind J Pharm Educ Res. 2020 Mar 3;54(2):284-92. doi: 10.5530/ijper.54.2.33.
105. Huang C, Peng L, Xu X, Lu Y, Wang X, Lan Z. Preparation and characteristics of a thermosensitive in situ gel loaded with chitosan nanoparticles for optimal ocular delivery of chloramphenicol. J Drug Deliv Sci Technol. 2023 Oct 14;89:104962. doi: 10.1016/j.jddst.2023.104962.
106. Hussain Z, Sahudin S. Preparation characterisation and colloidal stability of chitosan-tripolyphosphate nanoparticles: optimisation of formulation and process parameters. Int J Pharm Pharm Sci. 2016;8(3):297-308.
107. Shah VA, Patel JK. Optimization and characterization of doxorubicin loaded solid lipid nanosuspension for nose to brain delivery using design expert software. Int J Pharm Pharm Sci. 2021 May 1;13(5):45-57. doi: 10.22159/ijpps.2021v13i5.41137.
108. Jokubaite M, Marksa M, Ramanauskiene K. Application of poloxamer for in situ eye drop modeling by enrichment with propolis and balsam poplar buds phenolic compounds. Gels. 2024 Feb 21;10(3):161. doi: 10.3390/gels10030161, PMID 38534579.
109. Zirak MB, Pezeshki A. Effect of surfactant concentration on the particle size stability and potential zeta of beta carotene nano lipid carrier. Int J Curr Microbiol Appl Sci. 2014;4(9):924-32.
110. Russo E, Villa C. Poloxamer hydrogels for biomedical applications. Pharmaceutics. 2019 Dec 10;11(12):671. doi: 10.3390/pharmaceutics11120671, PMID 31835628.
111. Smail SS. Ex vivo irritation evaluation of a novel brimonidine nanoemulsion using the hen's egg test on chorioallantoic membrane (HET-CAM). Cureus. 2024 Aug 31;16(8):e68280. doi: 10.7759/cureus.68280, PMID 39350816.
112. Batista Duharte A, Jorge Murillo GJ, Perez UM, Tur EN, Portuondo DF, Martinez BT. The hen's egg test on chorioallantoic membrane: an alternative assay for the assessment of the irritating effect of vaccine adjuvants. Int J Toxicol. 2016 Oct 13;35(6):627-33. doi: 10.1177/1091581816672187, PMID 27733445.
113. Kapoor A. HET CAM irritancy study for development of gatifloxacin in situ gel formulation. Int J Adv Res. 2019 May 31;7(5):1218-25. doi: 10.21474/ijar01/9154.
114. McKenzie B, Kay G, Matthews KH, Knott RM, Cairns D. The hen's egg chorioallantoic membrane (HET-CAM) test to predict the ophthalmic irritation potential of a cysteamine-containing gel: quantification using Photoshop® and ImageJ. Int J Pharm. 2015 May 13;490(1-2):1-8. doi: 10.1016/j.ijpharm.2015.05.023, PMID 25980731.
115. Samimi MS, Mahboobian MM, Mohammadi M. Ocular toxicity assessment of nanoemulsion in-situ gel formulation of fluconazole. Hum Exp Toxicol. 2021 May 26;40(12):2039-47. doi: 10.1177/09603271211017314, PMID 34036827.